ChemComm

Accepted Manuscript

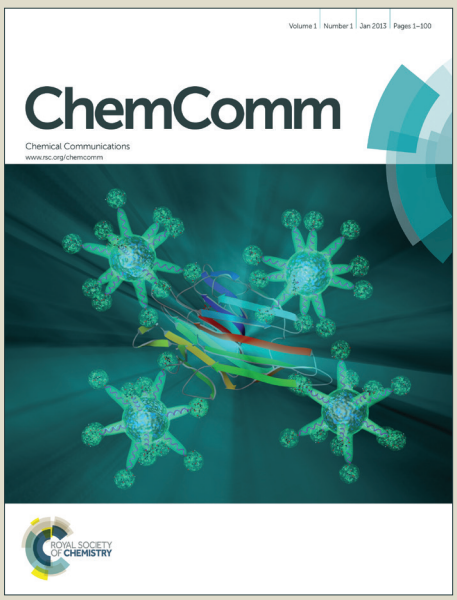

ROYAL SOCIETY OF CHEMISTRY

www.rsc.org/chemcomm

Journal Name

RSCPublishing

COMMUNICATION

Detection of microRNA SNPs with ultrahigh specificity by using reduced graphene oxide-assisted rolling circle amplification

Cite this: DOI: 10.1039/xoxxoooooox

Received ooth January 2012,
Accepted ooth January 2012

DOI: 10.1039/xoxxoooooox

www.rsc.org/

Xiaoli Zhu,[a] Yalan Shen,[a] Jiepei Cao,[a] Li Yin,[b] Fangfang Ban,[a] Yongqian Shu,[b,*] and Genxi Li,[a,c,*]

Here we report a reduced graphene oxide-assisted rolling circle amplification for the detection of miRNA SNPs. The difference of the signal of a miRNA SNP reaches 100 fold, a value over 10 times larger than some current methodologies, which allow the discrimination of a SNP even with naked eyes.

MicroRNAs (miRNAs) are endogenous non-coding RNAs with a length of 17-25 nucleotides (nt).[1] They play important regulatory roles in various normal and pathologic processes by targeting mRNAs for cleavage or translational repression.[2] Recent studies have also implicated miRNAs in a wide range of diseases including cancers, cardiovascular and cerebrovascular diseases, nervous system disease, etc.[3] The expression levels of some individual miRNAs may serve as promising diagnostic and prognostic biomarkers as well as new targets for therapy.[1,4]

Single nucleotide polymorphisms (SNPs) are important variations which may lead to phenotypes, traits, and diseases.[5] Because each miRNA may regulate hundreds of genes, miRNA SNPs especially those located in mature miRNAs (MIRs) can result in a high incidence of extensive cellular transformation and various diseases.[6] In recent decade, a number of miRNA SNPs have been defined and demonstrated to affect certain physiological processes or relate with many kinds of diseases.[7] For example, Duan et. al. found that mature miR-125a had a variant allele at the eighth nucleotide, which might significantly block the processing of pri-miRNA to pre-miRNA, in addition to reducing miRNA-mediated translational suppression.[7a] Jazdzewski et. al. otherwise reported that common SNP in pre-miR-146a decreased mature miRNA expression and predisposed to papillary thyroid carcinoma.[7b] Another study showed that mutations in the seed region of human miR-96 were responsible for nonsyndromic progressive hearing loss.[7c] To facilitate the access of various miRNA SNPs, Gong et. al. also created a miRNA SNPs database.[8] Despite of these previous efforts, it is believed that only a small part of miRNA SNPs has been revealed,[8] and a large amount of SNPs remains to be investigated.

Owing to the significance of miRNA in diagnosis and therapy, development of methodologies for the sensitive detection of miRNA is becoming a hot area.[9] Other than the efforts on the improvement of conventional biological tools (e.g. RT-PCR and Northern blot),[10] a variety of innovative methods including nanoparticles-based assays,[11] enzyme-linked assays,[12] isothermal amplification-based technologies,[13] etc, have also been developed. However, it is noted that detection of miRNA SNPs is rarely reported, despite of the importance of miRNA SNPs. Most of the reported miRNA SNPs were based on the detection of miRNA genes but not the miRNAs themselves. A main reason is the low ability of the current methodologies for the discrimination of single-base mutation of miRNAs. The high sequence homology among family miRNA members (e.g. let-7 family differs by only one or two nucleotides) and the small size of miRNA also make things harder. Though several fold difference of the signal between a wild miRNA and a single-base mutant can be achieved during the detection of miRNA in some reports,[14] a puzzle remains, that is whether the difference should be ascribed to a SNP or the repressed expression of the target miRNA. Therefore, a major challenge is to develop methods able to detect miRNAs with ultrahigh specificity.

Graphene has attracted a great research interest in biological applications.[15] It is also reported that graphene may improve the specificity for SNP genotyping.[16] However, unlike genomic DNA, miRNA has its intrinsic characteristics. Especially because the concentration of miRNA is very low (fM~pM level), the current graphene-based SNP genotyping methods cannot be simply transplanted for the detection of miRNA SNP owing to their unbalance between specificity and sensitivity. For example, Fan et. al. reported a graphene oxide (GO)-based chip for SNP genotyping.[16c] However, the required concentration of the target is in nM level, which is unsuitable for the detection of miRNA SNP. Here,

by adopting reduced graphene oxide (rGO) into a well-known isothermal amplification system, i.e. rolling circle amplification (RCA), we have developed a detection method with considerable sensitivity and ultrahigh specificity, which is able to detect miRNA SNPs. Mature miR-125a, a critical miRNA in breast cancer with a G-U polymorphism at the eighth nucleotide, and let-7 family, whose members differ by only one or two nucleotides (sequences shown in Table S1), have been adopted as models for this study. Moreover, in addition to the good discrimination of SNPs, the sensitivity as well as the usability can also be satisfactory, so this rGO-assisted RCA strategy might be a promising alternative for profiling miRNA SNPs in lab or clinic.

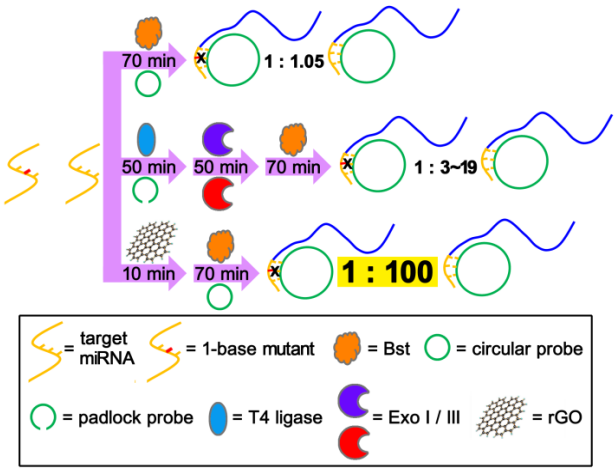

Scheme 1 Schematic presentation of the comparison of rGO-assisted RCA with conventional RCA and P-RCA in the specificity. In P-RCA, the scheme for the preparation of circular probe represents a routine method from published works;[17] the ratio of the signal intensity of a single-base mutant to a target is also cited from published works (Table S2).[14a,18]

RCA technique utilizes a circular single-stranded DNA probe as an everlasting template for DNA polymerization to generate multiple single-stranded linear copies of the original strand in a continuous head-to-tail series (Scheme 1). Once the original strand (usually the target) hybridizes with the circular probe, the polymerization is launched under the catalysis of polymerase and no longer depends on the original sequence. For this reason, the specificity of this early RCA model is poor. Our previous results showed that even a 5-base mutant variant (21 nt) might also be lengthened under RCA.[17] Here in this report, it is also shown that the difference between a single-base mutant and a wild sequence is only 1.0 to 1.05 (detailed data shown hereinafter). In order to improve the specificity, padlock probe-based RCA (P-RCA) was developed and became the most popular strategy till now.[19] In P-RCA, a padlock probe first hybridizes head-to-tail with a target nucleic acid sequence. The 3' and 5' ends of the probe are positioned adjacently and are sealed by a ligase, resulting in a circular probe with two ends connected. Non-circularized probe as well as the target sequence is removed by exonucleases, while the circularized probe may participate in RCA subsequently by introducing an extra linear primer (process shown in Scheme 1). A variety of strategies for the improvement of P-RCA have also been proposed in recent years.[18a,20] Table S2 shows the ability of the current P-RCA and some derivative methods for the discrimination of single-base mutation.[14a,18] The ratio of the signal intensity of a single-base mutant to a target is mainly concentrated in a range from 1:3 to 1:19, which is improved but still not satisfactory. Moreover, the improvement on the specificity is accompanied by the sacrifice of the simplicity and the time-efficiency. In our work, on the basis of RCA, we find that by incubating the miRNA (either the target or the variant) with appropriate amount of rGO for a certain period and followed by the proceeding of the routine RCA, the ratio can be elevated to 1:100 (Scheme 1, data shown hereinafter). The process is also simpler and more time-saving in comparison with P-RCA.

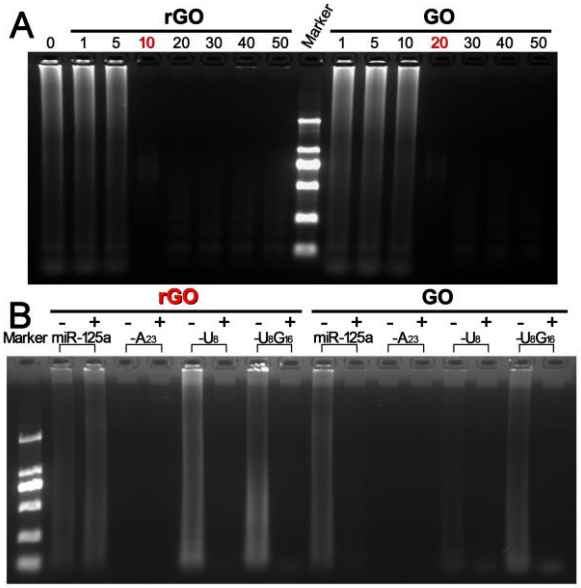

Fig. 1 Agarose gel electrophoresis patterns of RCA products in the presence of rGO or GO. (A) MiR-125a-U8 (1 μM) works as template. The numbers 1 to 50 indicate the concentrations of rGO/GO with a unit μg/ml. (B) Different variants of miR-125a (1 μM) work as templates. The symbols "+" and "-" indicate that rGO/GO is present and absent, respectively.

The methodology of rGO-assisted RCA was established after extensive trials. Briefly, a circular probe was first designed for the target miRNA (miR-125a or let-7a). That is, a single-base mismatched between the circular probe and the single-base variant (miR-125a-U8 or let-7c). To facilitate the production of fluorescent signals using SYBR Green I intercalator, a linear probe was also introduced to hybridize with the RCA products, and thus to make the RCA products double-stranded. Experimental details and the optimization of conditions have been shown in the Supporting Information (Fig. S1 and S2). Because rGO and GO have much in common, comparison of rGO with GO on the RCA of miRNA SNPs was made. Fig. 1A shows the agarose gel electrophoresis patterns of RCA products using miR-125a-U8 as the template. In the absence of either rGO or GO (the first lane), an apparent smear band throughout the lane characteristic of RCA products was observed,[21] confirming the poor specificity of the original RCA technique. With the increase of the quantity of either rGO or GO, the bands shadowed and disappeared, suggesting the inhibition on the amplification. Because high concentration of rGO/GO also inhibited the amplification of the target miR-125a (Fig. S3), a critical quantity of rGO (10 μg/ml) and GO (20 μg/ml) was adopted for further study. Under this critical quantity, amplification of miR-125a as well as miR-125a-U8 and some other imaginary mutants (miR-125a-A23: a single-base mutant at 3'-end, miR-125a-U8G16: a 2-base mutant) was measured. As is shown in Fig. 1B, the amplification of all the mutants were inhibited using either rGO or GO. In the presence of GO, the amplification of the target wild miRNA was also inhibited. So, rGO might be more suitable for the profile of miRNA SNP. 10 μg/ml of rGO was thereby adopted in the following experiments. It should also be noted that in the case of miR-125a-A23, no bands could be observed regardless of rGO/GO. It was because the catalysis of polymerase mainly depended on the base-paring at the 3'-end. So, the original RCA without using rGO/GO might be used for the detection of SNP only at the 3'-endmost base.

Some other techniques have also been adopted to characterize the rGO-assisted discrimination of miRNA SNPs. Atomic force microscope (AFM) results (Fig. S4) show that only in the presence of rGO, no amplified products could be observed, suggesting the good specificity of the rGO-assisted RCA. Real-time monitoring of the fluorescent signals have also been conducted by using a real-time PCR detection system. As is shown in Fig. 2A, the fluorescent signals increased with the amplification time in all the cases and reached a plateau after ca. 30 min. Without rGO, the curves for the amplification of the target miRNA (miR-125a) and its mutant miR-125a-U8 almost overlapped, whereas in the presence of rGO, a large gap between the signals could be observed. Characterization using fluorescence spectrophotometry and photography under UV-light at the terminal of RCA (30 min) also confirmed the real-time PCR results (Fig. 2B&C). The difference of the fluorescent signals in the presence of rGO for the detection of miRNA SNP reached 100 fold (15023 vs. 151, Fig. 2D), which could be easily distinguished by naked eyes and was the largest so far to our knowledge. Discrimination of another miRNA SNP using the rGO-assisted RCA was also achieved (Fig. S5 and S6). These results suggest that our strategy can be a universal approach for the discrimination of miRNA SNPs.

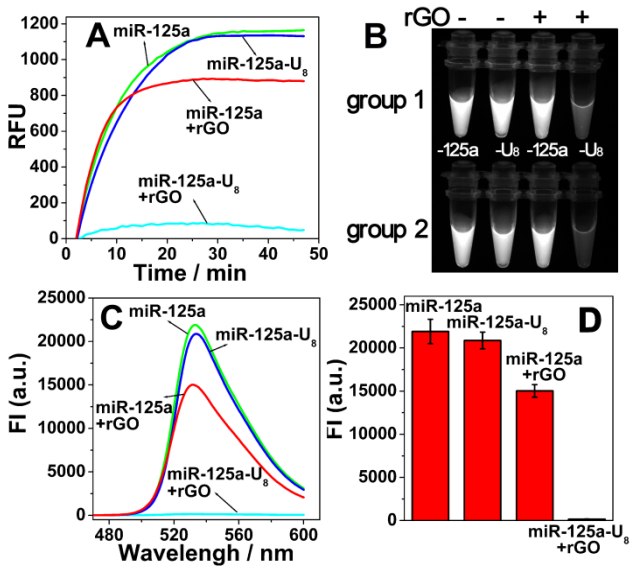

Fig. 2 (A) Real-time fluorescent signals of RCA in the presence or absence of rGO, and using miR-125a or miR-125a-U8 as the template. (B) Photograph of RCA products under UV-light. (C) Fluorescence spectra of RCA products. (D) Comparison of the fluorescence intensity of the peaks in (C).

The mechanism of the rGO-assisted RCA for the discrimination of miRNA was then studied. Electrophoretic results showed that only the pre-incubation of rGO with miRNA for a certain period might result in the discrimination of SNP (Fig. S7). No pre-incubation or the pre-incubation of rGO with other components of RCA (circular probe, dNTPs, or Bst DNA polymerase) had no effect on the improvement of the specificity of the subsequent RCA. Fourier transform infrared spectroscopic (FT-IR) results also showed that rGO only interacted with nucleic acids but not the enzyme (Fig. S8). In the previous report of Jia et. al., the GO-enhanced specificity of PCR was proposed to be ascribed to the interaction between GO and Pfu DNA polymerase.[16a] Here, it should be another mechanism that is responsible for our experimental phenomenon. Recently, Zhang et. al. reported that in comparison with the widely studied PEGylated GO, PEGylated rGO exhibited superior single stranded RNA loading and delivery capability.[22] By using computational simulation, they ascribed this capability to the stronger binding of the PEGylated rGO with the single stranded RNA. On the basis of this previous finding and our experimental results, we speculated that the strong binding of rGO with miRNA might rival the hybridization of the miRNA with circular probe. In the case of a target miRNA, the balance shifted to the miRNA- circular probe hybridization, whereas for the miRNA mutants, the miRNA-rGO binding dominated. Thus, rGO plays a key role for the regulation of the initiation of RCA.

Detection of miRNA was then performed. Fig. 3A shows that the fluorescent signals increase with the concentration of the target miR-125a. The curves of signal intensity vs. the concentration could be fitted by a sigmoidal equation. In the range from 10 fM to 100 pM, there is a linear relation. The detection limit is calculated to be 10.3 fM (3σ), which is favorable for the detection of miRNA in physiological conditions. As for the single-base mutant (miR-125a-U8), it could be seen from the electrophoresis patterns in Fig. S9 that no bands of RCA products were observed regardless of the concentration. Thus, by using this rGO-assisted RCA, it could be easy to discriminate whether there is a mutation on a specific miRNA for an individual. Various frequencies of miR-125a-U8/(miR-125a + miR-125a-U8) were also adopted to study the allele frequencies. It is observed from Fig. S10 that the increasing of the percentage of miR-125a-U8 leads to decreased fluorescent signals, and 5% of SNP can be differentiated.

In another case, two miRNAs with SNP may coexist, for example the let-7a and 7c of let-7 family. It is really a challenge to detect the actual concentration of them each, because another one may donate to considerable false positive signals if the specificity is not so good. In this work, let-7c with different concentrations (from 1 fM to 10 pM) was added into 100 fM let-7a to work as interference. The deviations of the measured values of let-7a are within 7.1% (Fig. S11). Given that system errors of max. 4.6% should also be taken into account, it can be concluded that there is little interference to the detection of let-7a even if excess let-7c is presented. Detection of let-7a in human lung cells was then performed. The content of let-7a is measured to be 4.1 × 10^9 copies/μg, which is slightly lower than some reported values.[14a,23] we consider the difference should be ascribed to the exclusion of the false positive of some interferences like let-7c, and our result may be closer to the real situation.

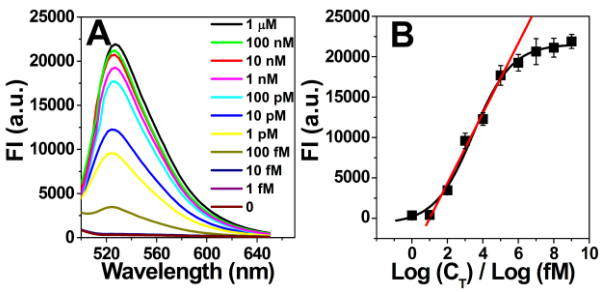

Fig. 3 Fluorescent detection of miR-125a by using the rGO-assisted RCA system. (A) The emission spectra of the amplified products using different concentrations of miR-125a as template. (B) Relationship between the peak fluorescence intensities of (A) and the corresponding concentrations of the target miRNA.

Conclusions

In summary, we have developed a novel rGO-assisted RCA strategy for the detection of miRNA SNPs. MiR-125a and let-7a together with their single-base mutants and some other variants are adopted as models for the detection. In comparison with conventional RCA and P-RCA techniques, the selectivity

of rGO-assisted RCA is greatly improved. The difference of the signals of miRNA SNPs reaches as high as 100 fold, which to our knowledge is the largest so far. As a result, miRNA SNPs could be detected directly even by naked eyes. Possible action mechanism of rGO has also been studied. The strong π-π stacking interaction between rGO and miRNA should be the main reason for the improved selectivity. Owing to the ultrahigh specificity, this rGO-assisted RCA strategy is a promising alternative for profiling miRNA SNPs in lab or clinic.

This work was supported by the National Natural Science Foundation of China (Grant No. 21235003, 61001035), the National Science Fund for Distinguished Young Scholars (Grant No. 20925520), and the Natural Science Foundation of Shanghai (14ZR1416500).

Notes and references

[a] Laboratory of Biosensing Technology, School of Life Sciences, Shanghai University, Shanghai 200444, P R China.

[b] Department of Oncology, the First Affiliated Hospital of Nanjing Medical University, Nanjing 210029, P R China. E-mail: shuyongqian@csco.org.cn

[c] State Key Laboratory of Pharmaceutical Biotechnology, Department of Biochemistry, Nanjing University, Nanjing 210093, P R China. E-mail: genxili@nju.edu.cn

† Electronic Supplementary Information (ESI) available. See DOI: 10.1039/b000000x/

1 B. Zhang, X. Pan, G. P. Cobb and T. A. Anderson, *Dev. Biol.*, 2007, **302**, 1-12.

2 H. Dong, J. Lei, L. Ding, Y. Wen, H. Ju and X. Zhang, *Chem. Rev.*, 2013, **113**, 6207-6233.

3 (a) G. A. Calin, C. Sevignani, C. D. Dumitru, T. Hyslop, E. Noch, S. Yendamuri, M. Shimizu, S. Rattan, F. Bullrich, M. Negrini and C. M. Croce, *Proc. Natl. Acad. Sci. U. S. A.*, 2004, **101**, 2999-3004; (b) M. V. Latronico, D. Catalucci and G. Condorelli, *Circ. Res.*, 2007, **101**, 1225-1236.

4 P. S. Mitchell, R. K. Parkin, E. M. Kroh, B. R. Fritz, S. K. Wyman, E. L. Pogosova-Agadjanyan, A. Peterson, J. Noteboom, K. C. o'briant, A. Allen, D. W. Lin, N. Urban, C. W. Drescher, B. S. Knudsen, D. L. Stirewalt, R. Gentleman, R. L. Vessella, P. S. Nelson, D. B. Martin and M. Tewari, *Proc. Natl. Acad. Sci. U. S. A.*, 2008, **105**, 10513-10518.

5 BS. Shastry, *Methods Mol. Biol.*, 2009, **578**, 3–22.

6 DP. Bartel, *Cell*, 2004, **116**, 281–297.

7 (a) R. Duan, C. Pak and P. Jin, *Hum. Mol. Genet.*, 2007, **16**, 1124-1131; (b) K. Jazdzewski, E. L. Murray, K. Franssila, B. Jarzab, D. R. Schoenberg and A. Dela Chapelle, *Proc. Natl. Acad. Sci. U. S. A.*, 2008, **105**, 7269-7274; (c) A. Mencia, S. Modamio-Hoybjor, N. Redshaw, M. Morin, F. Mayo-Merino, L. Olavarrieta, L. A. Aguirre, I. Del Castillo, K. P. Steel, T. Dalmay, F. Moreno and M. A. Moreno-Pelayo, *Nat. Genet.*, 2009, **41**, 609-613.

8 J. Gong, Y. Tong, H. M. Zhang, K. Wang, T. Hu, G. Shan, J. Sun and A. Y. Guo, *Hum. Mutat.*, 2012**,** **33**, 254-263.

9 S. Catuogno, C. L. Esposito, C. Quintavalle, L. Cerchia, G. Condorelli and V. de Franciscis, *Cancers*, 2011, **3**, 1877-1898.

10 (a) C. Potrich, V. Vaghi, L. Lunelli, L. Pasquardini, G. C. Santini, C. Ottone, M. Quaglio, M. Cocuzza, C. F. Pirri and M. Ferracin, *Lap Chip.*, 2014, **14**, 4067-4075; (b) A. Valoczi, C. Hornyik, N. Varga, J. Burgyan, S. kauppinen and Z. Havelda, *Nucleic. Acids. Res.*, 2004, **32**, e175.

11 S. W. Yang and T. Vosch, *Anal. Chem.*, 2011**,** **83**, 6935-6939.

12 K. K. Chan, Z. Liu, Z. Xie, M. Chiu, H. Wang, P. Chen, S. Dunkerson, M. Chiu, S. Liu, G. Triantafillou, R. Garzon, C. M. Croce, J. C. Byrd, N. Muthusamy and G. Marcucci, *AAPS. J.*, 2010, **12**, 556-568.

13 K. Wang, K. Zhang, Z. Lv, X. Zhu, L. Zhu and F. Zhou, *Biosens. Bioelectron.*, 2014, **57**, 91-95.

14 (a) H. Y. Liu, L. Li, L. L. Duan, X. Wang, Y. X. Xie, L. L. Tong, Q. Wang and B. Tang, *Anal. chem.*, 2013, **85**, 7941-7947; (b) L. Jiang, Y. Shen, K. Zheng and J. Li, *Biosens. Bioelectron.*, 2014**,** **61**, 222-226; (c) H. V. Tran, B. Piro, S. Reisberg, L. Huy Nguyen, T. Dung Nguyen, H. T. Duc and M. C. Pham, *Biosens. Bioelectron.*, 2014, **62**, 25-30.

15 (a) Y. J. Song, K. G. Qu, C. Zhao, J. S. Ren and X. G. Qu, *Adv. Mater.*, 2010, **22**, 2206-2210; (b) Z. W. Chen, Z. H. Li, J. S. Wang, E. G. Ju, L. Zhou, J. S. Ren and X. G. Qu, *Adv. Funct. Mater.*, 2014, **24**, 522-529; (c) M. Liu, J. P. Song, S. M.Shuang, C. Dong, J. D. Brennan and Y. F. Li, *ACS nano.*, 2014, **8**, 5564-5573.

16 (a) J. Jia, L. P. Sun, N. Hu, G. M. Huang and J. Weng, *Small*, 2012, **8**, 2011-2015; (b) M. Liu, H. M. Zhao, S. Chen, H. T. Yu, Y. B. Zhang and X. Quan, *Biosens and Bioelectron.*, 2011, **26**, 4213-4216; (c) J. Li, Y. Huang, D. F. Wang, B. Song, Z. H. Li, S. P. Song, L. H. Wang, B. W. Jiang, X. C. Zhao, J. Yan, R. Liu, D. N. He, and C. H. Fan, *Chem. Commun.*, 2013, **49**, 3125-3127.

17 X. L. Zhu, C. Feng, B. Zhang, H. Tong, T. Gao and G. X. Li, *Analyst.*, 2014, **140**, 74-78.

18 (a) Y. Q. Cheng, X. Zhang, Z. P. Li, X. X. Jiao, Y. C. Wang and Y. L. Zhang, *Angew. Chem. Int. Edit.*, 2009, **48**, 3268-3272; (b) Z. Zou, Z. H. Qing, X. X. He, K. M. Wang, D. G. He, H. Shi, X. Yang, T. P. Qing and X. X. Yang, *Talanta*, 2014, **125**, 306-312; (c) Z. Y. Tang, Y. Q. Cheng, Q. Du, H. X. Zhang and Z. P. Li, *Chinese Sci. Bull.*, 2011, **56**, 3247-3252; (d) Q. Wang, C. Y. Yang, Y. Xiang, R. Yuan and Y. Q. Chai, *Biosens. Bioelectron.*, 2014, **55**, 266-271; (e) A. Hatch, T. Sano, J. Misasi and C. L. Smith, *Genet. Anal.*, 1999, **15**, 35-40.

19 M. M. Ali, F. Li, Z. Q. Zhang, K. X. Zhang, D. K. Kang, J. A. Ankrum, X. C. Le and W. A. Zhao, *Chem. Soc. Rev.*, 2014, **43**, 3324-3341.

20 (a) J. S. Li, T. Deng, X. Chu, R. H. Yang, J. H. Jiang, G. L. Shen and R. Q. Yu, *Anal. Chem.*, 2010, **82**, 2811-2816; (b) Y. Q. Wen, Y. Xu, X. H. Mao, Y. L. Wei, H. Y. Song, N. Chen, Q. Huang, C. H. Fan and D. Li, *Anal. Chem.*, 2012, **84**, 7664-7669; (c) B. Yao, Y. C. Liu, M. Y. Tabata, H. T. Zhu and Y. J. Miyahara, *Chem. Commun.*, 2014, **50**, 9704-9706.

21 H. Kuhn, V. V. Demidov and M. D. Frank-Kamenetskii, *Nucleic Acids Res.*, 2002, **30**, 574-580.

22 L. M. Zhang, Z. L. Wang, Z. X. Lu, H. Shen, J. Huang, Q. H. Zhao, M. Liu, N. Y. He, Z. J. Zhang, *J. Mater. Chem B.*, 2013, **1**, 749-755.

23 G. Zhu, L. Liang and C. Y. Zhang, *Anal. Chem.*, 2014, **86**, 11410-11416.

